ISSN 2176-5480

22nd International Congress of Mechanical Engineering (COBEM 2013)
November 3-7, 2013, Ribeirão Preto, SP, Brazil
Copyright © 2013 by ABCM

AEROELASTIC ANALYSIS AND COMPARISON WITH IN-FLIGHT TESTING OF THE VECTOR-P UNMANNED AERIAL VEHICLE

David Fernando Castillo Zúñiga
Luiz Sandoval Góes
Technological Institute of Aeronautics (ITA), Comando-Geral de Tecnologia Aeroespacial (CTA), 12228-904 - São Jose dos Campos-SP-Brasil
davidfer@ita.br
goes@ita.br
Adolfo Gomes Marto
Roberto Gil Annes da Silva
Institute of Aeronautics and Space (IAE), Comando-Geral de Tecnologia Aeroespacial (CTA), 12228-904-São Jose dos Campos-SP-Brasil
agmarto@iae.cta.br
rasilva@iae.cta.br

Abstract. *This paper compares the computed numerical aeroelastic characteristics of the Unmanned Aerial Vehicle Vector-P with the in-flight testing identified modal characteristics. The Aircraft aeroelastic behavior is studied for different flight conditions. The modal parameters were obtained from experimental modal analysis using data from a Ground Vibration Test (GVT). A non-matched flutter analysis was performed to observe the evolution of aeroelastic damping and frequencies as a function of airspeed, and to understand coupling mechanisms. It was fixed a constant Mach number and a constant density for this analysis. The g-method for aeroelastic stability analysis was employed. Different aerodynamic modeling approaches were investigated such as the use of cruciform body models and flat plate projection. Based on information from the GVT a flight test planning was conducted. The data acquisition system is described. In order to identify the in-flight Vector-P modal characteristics, the Operational Modal Analysis (OMA) methodology was used. The Frequency Domain Decomposition (FDD) procedure was chosen, this technique is based on the Singular Valued Decomposition (SVD) of the power spectral densities of the only system output signals. The experimental results obtained by this methodology were compared with the predicted results supplied by GVT and the aeroelastic numerical models.*

Keywords: *UAV aeroelastic analysis, operational modal analysis, in-flight aeroelastic testing*

1. INTRODUCTION

Unmanned Aerial Vehicles (UAV) development is an actual top technological issue. These aircrafts have been used in recognizing missions, surveillance, mapping, etc. In the challenge to reach high altitudes and to have long endurance, the UAV projects and designs requires light weight structural configurations that results in a more flexible structure. The fact of not having a cockpit has given the possibility of new configurations that translate into new aerodynamic and structural designs. These innovative features create a strong need for aeroelastic evaluation.

The state of art of aeroelasticity's role in UAV design is described in (Weisshaar, 2001), where some interesting topics are aeroelastic tailoring and aeroelastic control. A classical aeroelastic analysis consists in determining previously the modal characteristics of the aircraft by means of an experimental modal test, or of a numerical Finite Element Method (FEM) analysis, or of both two. With the modal data as input a flutter analysis can be executed in order to know the critical operation conditions (Castilllo Zúñiga, 2009). The predicted aeroelastic behavior by the numerical o theoretical aeroelastic analysis should be verified or validated with wind tunnel tests or in-flight tests in actual operative conditions (Kitahara, 1981).

Suzus (2008) presented a numerical aeroelastic analysis of a composited material medium UAV using MSC FlightLoads® and Dynamics and the solver MSC NASTRAN® Aero 1. The UAV modal data was obtained through a FEM analysis. The flutter and divergence characteristics were presented and the effect of altitude and Mach number was examined.

Calvi e Vaccaro (2009) validated a numerical aeroelastic analysis for the SKY-Y UAV with in-flight test data. The UAV modal data was obtained from a FEM model updated with experimental modal results. Parametric flutter studies were presented.

Traditional Input/Output identification techniques are not easily carried out for aeroelastic systems in operative flight conditions because of the intrinsic difficulty on measuring actual input loads. Therefore, only the response output level should be desirably used for the identification of aeroelastic systems. This Ouput-Only approach is known as Operational Modal Analysis (OMA). Follador, *et al* (2009) showed that the OMA approach is a suitable methodology for aeroelastic modal parameter identification. In their work were applied the EFDD (Enhanced Frequency Domain Decomposition) identification method to identified the aircraft aeroelastic parameters from in-flight data.

ISSN 2176-5480

Mastroddi, *et al* (2010) applied an Output-Only, O-O approach to fixed wing UAV. The authors show how the use of the Output-Only, O-O approach allowed passively reducing the operative aeroelastic vibrations, via piezoelectric-patch devices (PZTs,) mounted aboard the UAV.

The determination of the aeroelastic behavior of an aircraft is crucial to ensuring a flight envelope free of aeroelastic instabilities. Similarly it is important to study whether the aeroelastic characteristics of a given configuration have influence on aerodynamic performance in flight dynamics and control system. The objective of this paper is to present the results of a numerical aeroelastic analysis for Vector-P UAV taking a modal information as input, product of modal Ground Vibration Test (GVT) and comparing these results with those obtained by operational modal analysis after collected aeroelastic in-flight test (Castillo Zúñiga, 2013).

The Vector-P is made mainly of composite material and it presents a relatively common configuration for vehicles of the same size, with an almost square fuselage, wing flaps with no dihedral, two vertical stabilizers, horizontal tail and a tail boom (Peña et al, 2011). The Vector-P specifications are shown in Tab.1.

Table 1. Unmanned Aerial Vehicle Vector–P Specifications.

Wingspan	2.6 m
Fuselage Length	1.525 m
Max Speed	185 Km/h
Engine	3 W 2-stroke reverse rotation gasoline engine.
Max Range	775 Km, depending on fuel on board
Cruise Speed	129 Km/h
Max Altitude	3 Km
Max Endurance	6 hours depending on fuel and payload on board
Max Takeoff Weight	34 Kg
Empty Weight	23 Kg
Max Fuel	12.3 liters
Fuel Per Hour	2.3 liters
Landing Speed	74 Km/h
Max Payload Weight	11.3 Kg, with fuel for one hour
Payload Vol. (Internal)	(225 x 225 x 685) mm

2. THEORETICAL BACKGROUND

2.1. Numerical aeroelastic model

The first and very important step to perform a numerical aeroelastic analysis is obtaining the aircraft modal Data. Castillo Zúñiga and Góes (2012) carried out a GVT for the Vector-P. The modal characteristics of the aircraft such as, resonance frequencies, modes shapes, structural damping, generalized mass and stiffness were determined. The authors simulated the actual flight conditions selecting a free-free GVT condition. The total configuration for the test had a weight of 31.5 kg.

The second stage is characterizing aerodynamically the aircraft. For this purpose, it was used the ZONA 6 method implemented in ZAERO software. This method is an unsteady finite element potential aerodynamic approach. Different modeling approaches were used for understanding the sensitivity in terms of aeroelastic stability behavior. Cruciform, flat plate with gap and flat plate only aerodynamic models were generated to identify the aeroelastic coupling mechanisms. The models describe above are presented in Fig. 1. The unsteady aerodynamic theoretical foundations such as modeling techniques including the procedures for aeroelastic stability analysis, known as g-method and ASE (Aeroservoelastic) open loop flutter analysis, are described in (Zona, 2008)

ISSN 2176-5480

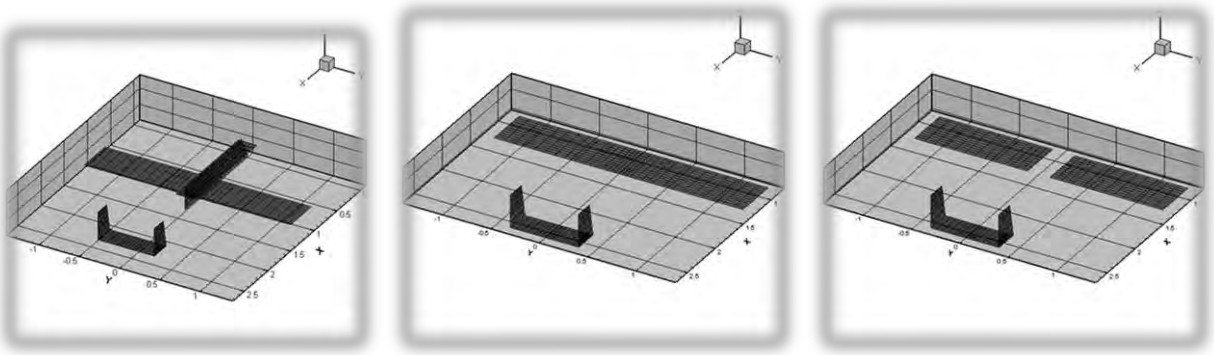

Figure 1. Cruciform, flate plate and flate plate with gap aerodynamic models.

2.2. Operational Modal Analysis (OMA)

The Operational Modal Analysis (OMA) is a parameter identification methodology based in only-output dynamic system approach. The techniques for OMA methodology can be formulated in time domain and frequency domain both (Follador et al, 2009). In this work was used the Frequency Domain Decomposition (FDD) technique described in (Gade et al, 2006).

The FDD technique is an extension of the Basic Frequency Domain (BFD), usually known as peak-picking technique. The first stage in this technique is to get the frequency content of the acceleration time responses, applying the Discrete Fourier Transform (DFT). For a specified sensor configuration, the Power Spectral Density (PSD) Matrix should be gotten. The size of the PSD matrix is n*n, n being the number of transducers. Each element of those matrices is a Spectral Density function. Cada elemento das matrizes é uma função de densidade espectral. The diagonal elements of the matrix are the real valued Spectral Densities between a response and itself (Auto Power Spectral Density). The off-diagonal elements are the complex Cross Spectral Densities between two different responses. All those matrices are Hermitian.

The FDD technique estimates the modes using a Singular Value Decomposition (SVD) of each of the spectral density matrices. This decomposition corresponds to a Single Degree of Freedom (SDOF) identification of the system for each singular value. The relationship between the input x(t) and the output y(t) can be written in the following form (Gade et al, 2006).

$$\boldsymbol{G}_{yy}(\omega) = \boldsymbol{H}(\omega)^{*}\, \boldsymbol{G}_{xx}(\omega)\, \boldsymbol{H}(\omega)^{T} \tag{1}$$

where $\boldsymbol{G}_{xx}(\omega)$ is the input Power Spectral Density (PSD) matrix. $\boldsymbol{G}_{yy}(\omega)$ is the output PSD matrix, $\boldsymbol{H}(\omega)$ is the Frequency Response Function (FRF) matrix, and * and the superscript T denotes complex conjugate and transpose, respectively. The FRF matrix can be written in a typical partial fraction form, in terms of poles, λ_k and residues, R_k:

$$\boldsymbol{H}(\omega) = \frac{\boldsymbol{Y}(\omega)}{\boldsymbol{X}(\omega)} = \sum_{k=1}^{m} \frac{\boldsymbol{R}_k}{j\omega - \lambda_k} + \frac{\boldsymbol{R}_k^{*}}{j\omega - \lambda_k^{*}} \tag{2}$$

with

$$\lambda_k = -\sigma_k + j\omega_{dk} \tag{3}$$

where m is the total number of modes of interest, λ_k being the pole of the k[th] mode, σ_k the modal damping (decay constant) and ω_{dk} the damped natural frequency of the k[th] mode.

Using Eq. 1 for matrix $\boldsymbol{G}_{\boldsymbol{yy}}(\omega)$ and Heaviside partial fraction theorem for polynomial expansions, we obtain the following expression for the matrix output PSD matrix $\boldsymbol{G}_{\boldsymbol{yy}}(\omega)$ assuming the input is random in both time and space and has a zero mean white noise distribution, i.e. its PDS is a constant, i.e. $\boldsymbol{G}_{\boldsymbol{xx}}(\omega) = \boldsymbol{C}$:

$$\boldsymbol{G}_{yy}(\omega) = \sum_{k=1}^{m} \frac{\boldsymbol{A}_k}{j\omega - \lambda_k} + \frac{\boldsymbol{A}_k^{*}}{j\omega - \lambda_k^{*}} + \frac{\boldsymbol{B}_k}{-j\omega - \lambda_k} + \frac{\boldsymbol{B}_k^{*}}{-j\omega - \lambda_k^{*}} \tag{4}$$

Considering a lightly damped model where the contribution of the modes at a particular frequency is limited to a finite number (usually 1 or 2), the response spectral density matrix can then be written as the following final form:

ISSN 2176-5480

$$\boldsymbol{G}_{yy}(\omega) = \sum_{k \epsilon Sub\,(\omega)} \frac{d_k \boldsymbol{\psi_k} \boldsymbol{\psi_k}^{\boldsymbol{T}}}{j\omega - \lambda_k} + \frac{d_k{}^{*} \boldsymbol{\psi_k}^{*} \boldsymbol{\psi_k}^{*\boldsymbol{T}}}{j\omega - \lambda_k{}^{*}} \quad (5)$$

where $k \epsilon Sub\,(\omega)$ is the set of modes that contribute at the particular frequency and where ψ_k and d_k are modal shape and the scale factor of the k^{th} mode respectively.

This final form of the matrix is then decomposed into a set of singular values and singular vectors (where the singular vectors are approximation of the modal shapes) using the SVD technique . This decomposition is performed to identify single degree of freedom models of the problem. The spectral density matrix is approximated to the following expression after SVD decomposition:

$$\boldsymbol{G}_{yy}(\omega) = \boldsymbol{\Phi \Sigma \Phi}^{T} \quad (6)$$

$$\boldsymbol{\Phi \Phi}^{T} = \boldsymbol{I} \quad (7)$$

where Σ being the singular value matrix, and Φ the singular vectors matrix:

$$\boldsymbol{\Sigma} = diag(s_1, \ldots\ldots, s_r) \quad (8)$$

$$\boldsymbol{\Phi} = [\{\phi_1\}\{\phi_2\}\{\phi_3\}\ldots\{\phi_r\}] \quad (9)$$

were ϕ_i are approximations of the individual mode shapes. The number of nonzero elements in the diagonal of the singular matrix corresponds to the rank of each spectral density matrix. The singular vectors correspond to an estimation of the mode shapes and the corresponding singular values are the spectral densities of the SDOF system expressed in Equation (14). This technique allows us to identify possible coupled modes that are often indiscernible as they appear on the spectral density functions. If only one mode is dominating at a particular frequency, then only one singular value will be dominating at this frequency. In the case of close or repeated modes, there will be as many dominating singular values as there are close or repeated modes (GADE et al, 2006)..

3. FLIGHT TEST AND ANALYSIS PROCEDURES

3.1. Data acquisition system and accelerometers placement

The data acquisition system for flight test of the Vector-P consists of an embedded control system (CompactRIO), accelerometers, GPS, inertial unit, pressure sensor and actuators. CompactRIO is a reconfigurable embedded control and acquisition system. The CompactRIO system's rugged hardware architecture includes I/O modules, a reconfigurable FPGA chassis, and an embedded controller. The accelerometers used for data acquisition were of DC type (PCB) with low frequency band response (0-100 Hz) with ±10 m s-2 amplitude range and high sensitivity 200 mv/g . The choice of positioning for the accelerometers in flight test was based on two objectives: to have a point of comparison with the results of experimental modal analysis (GVT), and to identify the modes that would have predominance in any aeroelastic instability, according to the results of numerical aeroelastic analysis. A total of 6 accelerometers were used, and their placement is presented in Fig. 3.

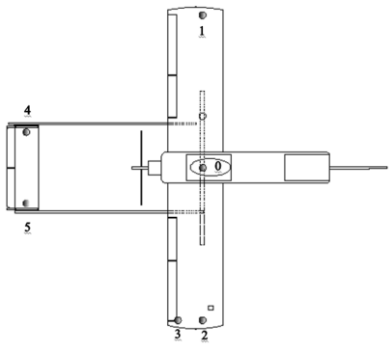

Figure 3. Accelerometers positioning in the airframe.

3.2. Flight test manouvers and spectral parameters

For the planning of the flight test maneuvers required for operational modal analysis were taken into account the following features of the flight envelope of Vector-P: maximum operating speed (51.4 m / s) and cruising speed (35.8 m/s). The following range of speeds chosen in order to cover the entire flight envelope of the Vector-P: 25, 30, 35, 40,

ISSN 2176-5480

45, 50 m/s.. The goal of each maneuver was to keep fixed flight condition, leaving the aircraft under atmospheric disturbance. The duration of each operation for a certain speed was set at 120 s.

PSD matrices were calculated using the responses of the six accelerometers for each flight condition by means of . Welch methodology. used to calculate the PSD matrices. With a sample frequency of 1000 Hz, a hanning window was used having a overlap de 50% resulting in a spectral resolution of 0.24 Hz. The Frequency Domain Decomposition was applied for each PSD matrix correspondent to the each flight condition. After computing these modal parameters, extracted from the aeroelastic flight test, they were compared with the same parameters estimated from the aeroelastic analysis.

4. RESULTS

4.1. Numerical aeroelastic analysis results

Some important modal characteristics of the aircraft such as, resonance frequencies and structural damping are shown in Tab. 2. Figure 4 presents the modal modes interpolated to the panel aerodynamic mesh.

Table 2. Identified natural modes characteristics.

Mode	Frequency (Hz)	Damping (%)
1st Symmetric Tail-Booms Bending Mode	7.56	1.45
1st Anti-symmetric Tail- Boom Bending Mode	8.67	2.02
1st Symmetric Wing Bending Mode	10.3	1.72
1st Anti-symmetric Wing Bending Mode	21.7	1.55
2nd Asymmetric Bending Mode	34.6	4.10
1st Anti-symmetric Torsional Mode	49.5	3.67
1st Anti-symmetric Torsional Mode	55.2	4.32

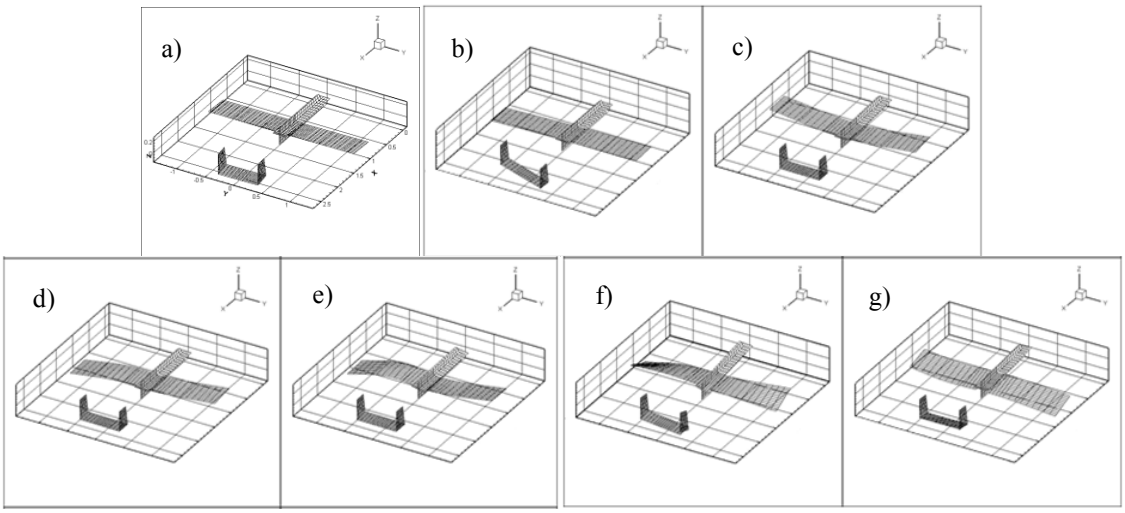

Figure 4. Interpolated vibration modes: a) 7.56 b) 8.67 Hz c) 10.3 Hz d) 21.7 Hz e) 34.6 Hz f) 49.5Hz g) 55.2 Hz

For a Mach number set at 0.1, and the air density of 1090 kg/m3 for air, a VGF diagram is shown in Fig. 5. It It is shown the variation of frequencies and the associated damping modes with respect to airspeed. In this case the g-method was employed . In this diagram, it can be appreciated how flutter critical condition appears at a velocity of 256.9 m/s at a frequency of 15.8 Hz Note how the mode that crosses the threshold of zero damping is linked to the second mode bending asymmetric booms, but this coalescence process are influencing the first three modes.

ISSN 2176-5480

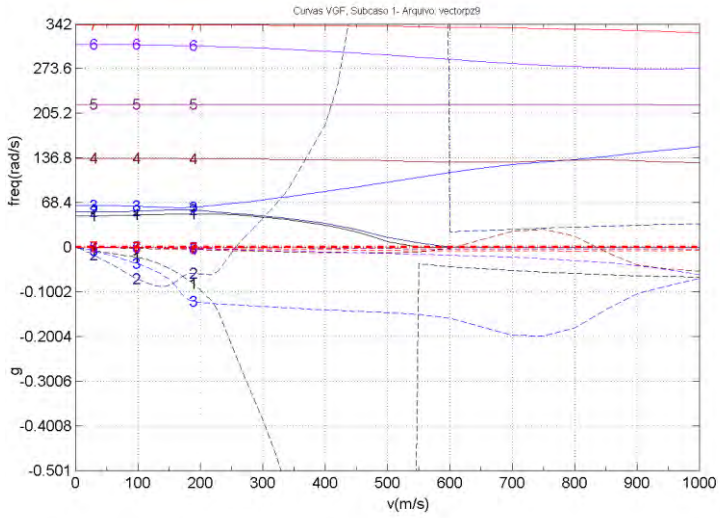

Figure 5. V-g-f diagram: Mach =0.1, H= 1100m, g-method.

4.1.1. Effect of the aerodynamic fuselage representation

We compared three representations for aerodynamic fuselage representation. For a Mach number set at 0.1, and the density of air at 1,090 kg/m^2, it was obtained the results presented in Tab. 4 using the g-method. The cruciform model takes into account the influence of the fuselage in the other airfoils. It can be observed that, compared with the flat plate model the model cruciform slightly elevate the critical flutter speed. It highlights the biggest difference with respect to the other two representations of the model with a gap between the semiwings. This reaffirms the care that must be taken not to use this type of representation due to the distortion generated by the false vortex created by the discontinuity.

Table 4. Flutter boundaries for the different aerodynamic fuselage representations.

Fuselage Representation	V_f [m/s]	F_f [Hz]
Cruciform	256.95	8.15
Flat Plate with gap	264.167	8.08
Flat Plate	252.99	8.23

4.1.2. Effect of the altitude

In order to know the dependence of the Vector-P flutter boundary with altitude it was performed analyses for different values of altitude. The g-method and ASE open-loop method were used. Table 5 shows the flutter boundaries for the different altitudes and their corresponding densities.

Table 5. Flutter boundaries for different altitudes

		g-method		**ASE Method**	
Altitude	**Density** (Kg/m^3)	$\mathbf{V_f}$ (m/s)	$\mathbf{f_f}$ (Hz)	$\mathbf{V_f}$ (m/s)	$\mathbf{f_f}$ (Hz)
Sea level	1.225	246.60	8.11	241.11	8.14
1100 m	1.090	256.95	8.15	251.98	8.18
2000 m	1.004	265.56	8.17	260.65	8.19
3000 m	0.907	277.23	8.18	271.95	8.21

We observed very similar results for both methods which emphasizes that both the critical velocity of flutter as the frequency associated increase as the altitude increases. The variation of the flutter boundary is illustrated in Fig. 6 which shows that the boundary marked by the ASE method is a bit more conservative.

ISSN 2176-5480

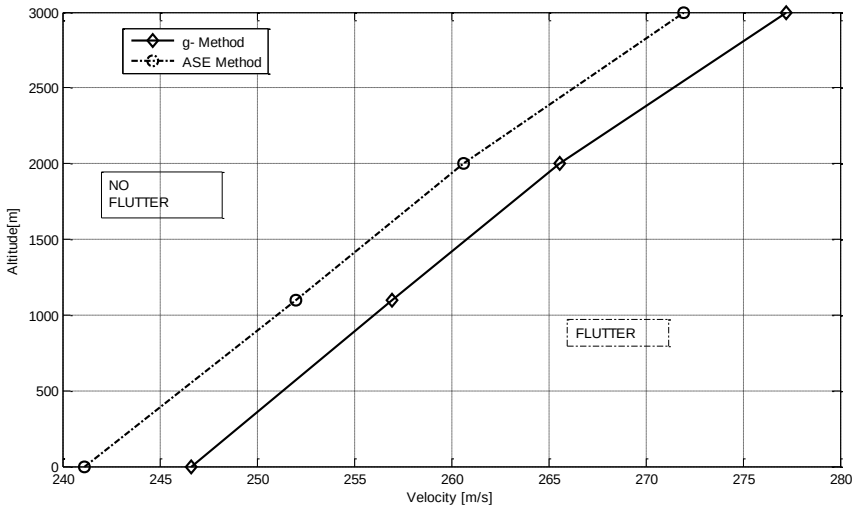

Figure 6. Flutter variation with Altitude

4.2 Operational modal analysis results

The data were analysed using the MATLAB® software for identifying modal parameters through FDA/OMA techique. Figure 7 shows the variation main and second singular values with respect to the airspeed. The main singular value points two relevant peaks. It is observe that in their respective frequency these modes are the only dominant . It is not observed a clear change in the frequency dependence of the speed. The small variations in frequency are the result of the modal frequencies dependence of the mass configuration of the aircraft, the limitations of the spectral resolution, and the influence of noise.

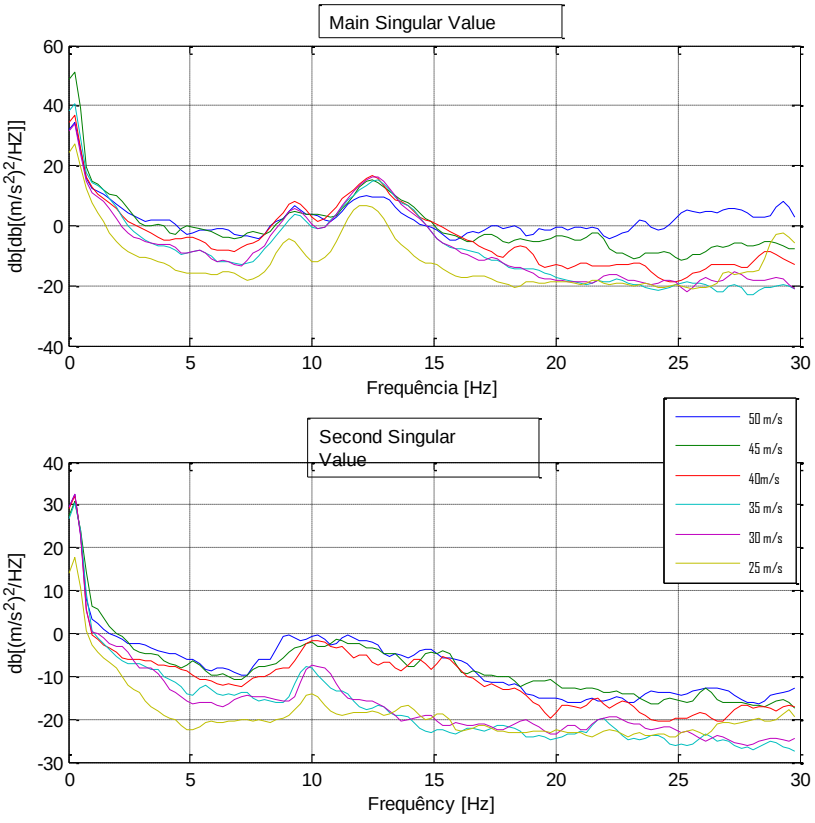

Figure 7. First and second singular values for each velocity

ISSN 2176-5480

The identified modes of vibration including frequency and damping factors for each airspeed are shown in Table 6. For most airspeeds the first resonant frequency appears around 9.28 Hz and the second around 12. 45 Hz. It is observed variations in resonant frequency corresponding to the second mode for some speeds. The variations do not show a tendency indicating a change in structural modes as function of airspeed. The variations in modal frequency can be explained by the in-flight mass configuration variation and in part by the limitations in resolution of the spectral analysis. The identified modal dampings did not show great changes in dependence on the airspeed that indicated some instability. The damping calculated here assumes the peak singular value being proportional to the main peaks of the FRFs equivalent. The noise and low spectral definition at some speeds do not allow estimating modal damping.

Table 6. OMA/ In-flight test identified modal charateristics.

	1st Symmetric Tail-Booms Bending		1st Wing Bending	
Velocity (m/s)	**Frequency [Hz]**	**Damping (%)**	**Frequency[Hz]**	**Damping (%)**
50	9.28	-	12.21	-
45	9.28	-	12.45	4.47
40	9.28	5.05	12.45	4.02
35	9.28	5.39	12.69	4.34
30	9.28	5.05	12.45	4.77
25	9.03	4.58	12.21	4.93

Figure 8 shows the modes shapes corresponding to the tail-booms 1st bending mode and the 1s bending mode wing. The modes have a good relationship with the analogous modes identified in GVT allowing you to check your mail. For the tail-booms 1st bending mode is observed a vertical displacement of the empennage while the movement of the wing is less significant.

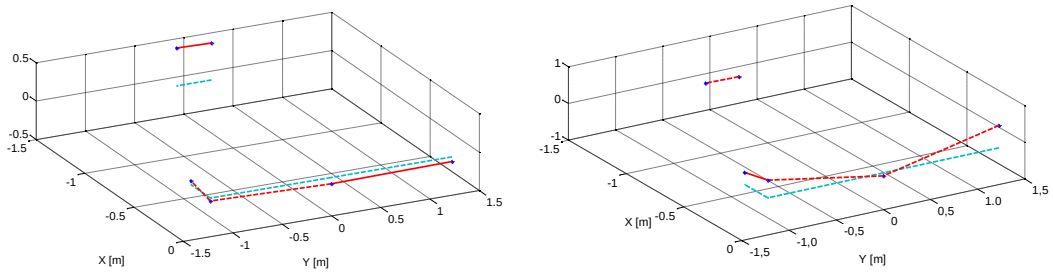

Figure 8. OMA Identified natural modes:tail-booms bending and wing bending.

5. COMPARISON BETWEEN NUMERICAL AND EXPERIMENTAL AEROELASTIC RESULTS

Figure 9 shows a V-g-f diagram with the comparison between the results of the numerical aeroelastic analysis and experimental aeroelastic flight test/OMA analysis. Observing the part corresponding to the frequency is observed an offset between the numerically estimated frequencies (ranging from the frequencies identified in GVT) and the frequencies identified from the in-flight test. This difference in the value for frequency is caused by the lower mass of the aircraft in flight test with respect to the GVT. The most important for comparison associated with the trends of variations of those frequencies with respect to speed. Observing the variation between the frequencies identified the flight test validates the trend predicted by numerical analysis. In this analysis the frequencies associated with these two modes kept themselves less dependent on the speed within the flight envelope of Vector-P, not yet having no phenomenon of coalescence between them.

ISSN 2176-5480

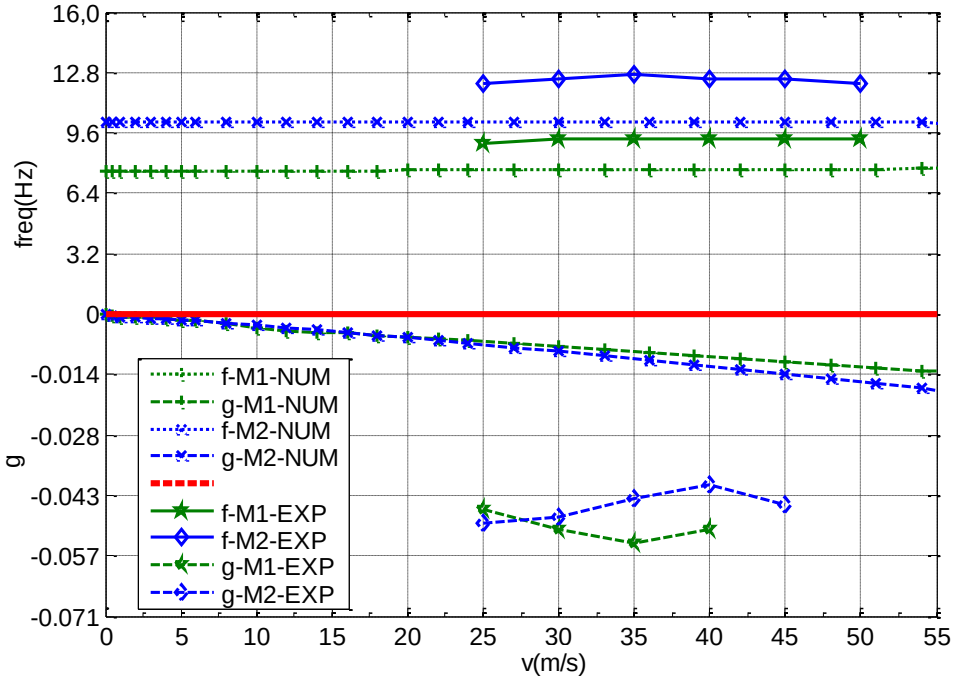

Figure 9. V-g-f diagrams comparising numeric and experimental.

Concerning to the modal aeroelastic damping, it can be seen higher magnitudes associated to the flight testing/ OMA identified modes. This off-set is related to the available structural damping that in the numerical analysis is not taken into account. The damping for these two modes identified from GVT ware around 2%. We see that for the flight test was between 4 and 5.4%. The natural tendency away from critical speed is that the aeroelastic damping increases with increasing speed. Although reflect the characteristics of available structural damping highlighted above, the damping identified by the method of bandwidth proved to be much influenced by the spectral resolution and the definition of the frequency peaks.

6. CONCLUTIONS

It was possible to characterize aeroelastically the Vector-P flight envelope. The characterization was done by means of an aeroelastic numerical analysis based in only experimental modal information (GVT), and compared with flight test/OMA using only the modal responses of the system. The trends of the modal frequencies as a function of velocity predicted numerically were validated with OMA results. It was found that there are aeroelastic instabilities in the Vector-P flight envelope.

The FDD/OMA technique proved to be very useful for identification of resonant frequencies given the ability to point to the modes that dominate in specific frequency. It was observed limitations in the estimation of modal damping and therefore it is advisable to estimate this parameter with other techniques.

7. ACKNOWLEDGEMENTS

This work was supported in part by CNPq-Conselho Nacional de Desenvolvimento Científico e Tecnológico – Brasil. The Authors of this paper would like to acknowledge Professor Airton Nabarrete Ph.D., Eng. Jany Lima, Eng. Jonatas Sant´Anna M. Sc. and all who contributed in some way for this work.

8. REFERENCES

Calvi, N. and Vaccaro, V., 2009. "Flutter flight test and aeroelastic model validation of UAV SKY-Y". In Proccedings of the 20st Congresso Nazionale Associazione Italiana Di Aeronautica E Astronautica. Milan, Italy.

Castillo Zúñiga, D. F., 2009. "Subsonic Wing Aircraft FlutterAnalysis ". Degree Final Work (Mechanical Engineering) - Universidad del Valle, Cali, Colombia.

Castillo Zúñiga, D. F. and Góes, L. C. S., 2012. "Modal Testing of the Vector-P Unmanned Aerial Vehicle" . In *Proccedings of the 7th Brazilian Congress of Mechanical Enginnering - CONEM2012.* São Luiz de Maranhão, Brazil.

ISSN 2176-5480

Castillo Zúñiga, D. F.,1981 —Aroelastic Analysis and Comparison with In-Flight Testing of Unmanned aerial Vehicles". Master thesis (Flight Mechanics and Control) - Instituto Tecnologico de Aeronáutica, São Jose dos Campos, Brazil.

Follador, R.., De Souza, C. E., Marto, A. G., Da Silva, R. G. A. and Góes, L. C. S., 2009. –Comparison of in-fligth measured and computed aeroelastic damping: modal identification procedures and modeling approaches". In *Proccedings of the International Forum On Aeroelasticity And Structural Dynamics* - IFASD2009, Seattle, USA.

Kitahara, W. T.,1981. –Medium aircraft in-Flight flutter testing". Final degree work (Aeronautic Engineering) - Instituto Tecnologico de Aeronáutica, São Jose dos Caampos, Brazil.

Mastroddi, F., Coppotelli, G. and Cantella, A., 2010. –Aeroelastic identification of a flying UAVs by output only data with applications on vibration passive control". In *Proccedings of the 51st AIAA/ASME/ASCE/AHS/ASC Structures, Structural Dynamics And Materials Conference*. Orlando, USA.

Peña, D. C. B., Góes, L. C. S., Santos, J. S. and Guzman, L. E. S., 2011. –Implementation and validation of a micropilot control system for Vector-P aircraft in flight level". In *Proccedings of the 9st Latin American Robotics Symposium, And Ieee Colombian Conference On Automatic Control*. Bogota, Colombia.

Suzus, U., 2008. –Aeroelastic analysis of an unmanned aerial vehicle". Thesis (M.Sc in Mechanical Engineering) - Middle East Tecnhical University, Ankara.

Weisshaar, A. T., Nam, C. and Batista Rodriguez, A., 1998. –Aeroelastic tailoring for improved UAV performance". In *Proccedings of the 39st AIAA Structures, Structural Dynamics, And Materials Conference*. Long Beach, USA.

Weissharr, T. A., 2001. –Aeroelasticity's role in innovative UAV design and optimization—the way things ought to be". In *Proccedings of the 41st Annual Israel Conference On Aerospace Sciences*. Tel Aviv and Haifa, Israel.

ZONA Technology. ZAERO theoretical manual. Scottsdale, 2008.

9. RESPONSIBILITY NOTICE

The authors are the only responsible for the printed material included in this paper.